International Journal of Scientific Research in Computer Science, Engineering and Information Technology
© 2018 IJSRCSEIT | Volume 3 | Issue 8 | ISSN : 2456-3307
DOI : https://doi.org/10.32628/CSEIT1838106

Human Gait Indicators of Carrying a Concealed Firearm : A Skeletal Tracking and Data Mining Approach

Henry Muchiri*[1], Ismail Ateya[2], Gregory Wanyembi[2]

*[1]Faculty of Information Technology, Strathmore University, Nairobi, Kenya

[2]Faculty of Information Technology, Strathmore University, Nairobi, Kenya

[3] School of Computing and Informatics / Mount Kenya University, Thika, Kenya

ABSTRACT

There has been an increase in crimes involving illegal firearms in the last couple of years. Previous studies have found that most illegal firearms are carried in a concealed manner. The detection therefore of persons carrying concealed firearms is critical in maintaining security especially in public places. Literature indicates that disruption in gait is a major indicator used by security personnel to detect persons carrying concealed firearms especially those tucked on the hip. However, the specific gait parameters that are indicative have not yet been quantitatively determined. The purpose of this study therefore is to analyze the gait of persons carrying a concealed firearm tucked on the right hip and to quantitatively determine the gait characteristics associated with carrying the firearm. A simulation of persons walking while carrying a concealed firearm and when unarmed was recorded using Kinect V2 depth camera. The depth camera provided 3D spatial skeletal joint position features of tracked joints for the armed and unarmed scenario. Paired t-tests were conducted to compare these features. Further, the results of the t-tests were related to the anatomical planes of Motion. Results showed that persons carrying a firearm demonstrated disrupted gait characterized by right arm abduction, left arm adduction, right leg adduction and extension. These findings extend existing gait indicators which can be employed by security personnel to identify persons carrying concealed firearms.

Keywords : Behavioral Indicators of Concealed Weapon, Concealed Weapon Detection, Feature Ranking, Human Skeletal Tracking.

I. INTRODUCTION

Incidences involving illegal firearms have been on the rise in the past couple of years worldwide. This has become a major concern for security agencies. According to the gun violence archive, there has been a steady increase in firearm related incidences between the years 2014 and 2017 in the United states of America as illustrated by fig. 1 [1]. In Kenya, the national police service annual crime report indicates that over a third of all criminal offences in major towns in the country involved the use of a firearm [2]. Several Studies by [3], [4] , [5] point out that most illegal firearms are carried in a concealed manner.

It's against this backdrop that the detection of persons carrying concealed firearms has become paramount in maintaining security in public places [6].

Various concealed firearm detection techniques have been adopted. One is by use of trained law enforcement personnel and CCTV operators in CCTV-mediated surveillance who lookout for certain indicators to identify persons carrying concealed firearms.

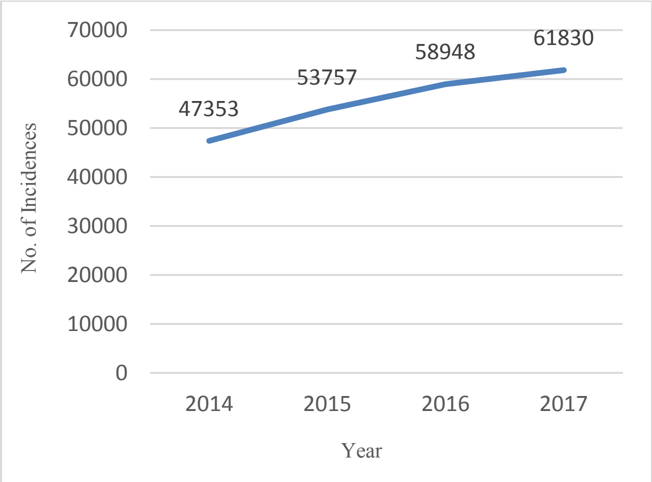

Figure 1. Incidences Involving Firearms in the US

Broadly, these indicators are classified into two; behavioural indicators and presence indicators. Behavioural indicators are the body language of a person carrying a weapon while presence indicators are indicators from the weapon itself. Example bulges, sagging of clothing etc.

Studies by [7], [8], [9] found that people carrying concealed firearms normally exhibit certain behavioral or body language indicators that trained law enforcement personnel and CCTV operators use to detect them. A study by [7] did a psychophysical experimental to determine the visual cues used by the operators. The study found that there was a significant positive correlation between the perceived level of dysphoria and the degree to which the gait and the posture of the target were used by the operators to detect a concealed firearm.

According to [3], [4] , [5], most illegal firearms are tucked on the hip without a holster to facilitate easier access. This is specifically, on the right and back side of the hip and crotch areas. In addition, [3] notes that when a firearm is tucked on the hip, it changes the gait of the person by hindering leg movements and consequently resulting in a disrupted stride and shortened arm swing as the individual attempts to either conceal the weapon or limit its movement so as not to drop it.

The Previous studies described above used qualitative research techniques to determine the behavioural indicators of carrying a concealed firearm from CCTV operators. This approach is subjective and does not give measurable indicators. The aim of this study, therefore, is to extend the findings of these studies by quantitatively analysing the gait of persons recorded on video carrying a concealed firearm tucked on the right hip and statistically measuring and determining the gait characteristics that are indicative.

This will be achieved by tracking the human skeletal joints and extracting the spatial characteristics and finally using feature selection algorithms in data mining to determine the changes in the skeletal body joints. Numerous studies have been conducted by analysing changes in skeletal body joints. For instance, a study by [10] used the skeletal data to determine gender, studies by [11], [12], [13], [14] used the data for activity recognition, a study by [15] used skeletal joint data to distinguish between patients suffering from Parkinson's disease and a study by [16] used skeletal joint data for fall detection in elderly persons who live alone.

The gait indicators in this study can be used by law enforcement and CCTV operators to identify persons carrying concealed firearms. In addition, studies by [7], [17] have recommended automation to improve CCTV-mediated surveillance for concealed firearm detection due to inherent challenges such as task interruptions, visual overload and operator fatigue which may result in errors. The determination of gait characteristics in this study will provide the necessary quantifiable data that can be used to train and develop machine learning models.

II. RELATED WORKS

This section will review related studies and approaches that have been used to determine the behavioural indicators of persons carrying a concealed firearm on their body.

A study by [9] employed a psychophysical experiment using a signal detection framework to determine the CCTV operator performance in detecting firearms concealed on a human body. The operators were provided with mock CCTV footage containing four scenarios; a person carrying a visible and concealed firearm, and a visible and concealed innocuous object which had similar characteristics to a firearm. The operators were required to determine whether a signal (firearm) was present or absent in the footage. After performing the firearm detection task, the frequencies with which various strategies were used by CCTV operators in the detection task were elicited through a questionnaire. This was correlated with firearm detection performance to determine the strategies associated with effective gun detection. In the concealed condition, the strategies used by participants were elicited by asking them to rate a series of statements which were tailored to the concealed condition. These conditions were related to gait, facial expressions, posture and demeanour.

The study found that the sensitivity to a concealed firearm was significantly lower than sensitivity to an unconcealed firearm. Further, sensitivity to a concealed firearm was below zero, indicating that ability to distinguish between a concealed firearm and a concealed bottle was below chance. The paper concluded that based on the experimental conditions, it was not possible to derive effective strategies for the detection of concealed firearms.

Another study by [7] investigated whether CCTV operators were able to perceive differences in emotional states and non-verbal behaviour of people in two categories of mock videos containing people who were carrying concealed firearms and people who were carrying an innocuous item. A cue-detection questionnaire was used to obtain information about characteristics of the targets' movement pattern in order to understand how carrying a gun affected the appearance of the carrier to the observer in terms of cues related to the carrier's emotional state.The movement pattern was specified by eight characteristics which included stride length, arms' swinging, heavy footedness,speed,degree of fluidity, rigidity, and and degree of exaggeration.

The study used Pearson's correlation and found a significant positive correlation between the level of dysphoria-unease and the degree to which the gait and the posture and specifically degree of arm swinging of the target were used by observers in order to gain an impression of the targets' affective state while a significant negative correlation was found between the level of perceived dysphoria and the degree to which the facial expressions of the target were used by observers in order to gain an impression of the targets' mood.

III. METHODS AND MATERIAL

A. Participants

A total of 26 participants consisting of 19 male and 7 female undergraduate students with a mean age of 20.0 ± 1.3 years, were included in the study. General study group characteristics are as shown in table 1.

The participants were selected using non-probabilistic convenience sampling technique. participants who reported any injury or deformity that affected their motion were excluded. The study was approved by the Strathmore University institutional ethics review committee (SU-IERC) (Certificate number SU-IRB 0246/18, dated 05.07.2018). A written consent was obtained from all participants prior to study procedures.

Table 1. Participants demographic characteristics.

	Mean ± standard deviation
Age (Years)	20.0 ±1.3
Height (Meters)	1.7 ± 0.1
Weight (Kg)	65.8 ± 13.0

B. Materials

1) **Kinect V2 Sensor:** Microsoft Kinect V2 is a low-priced motion sensor which uses the time of flight measurement principle. The Kinect V2 is an improvement of the Kinect V1 which uses the structured light principle and has been found to have low accuracy and resolution [18]. Microsoft Kinect V2 integrates three sensors into a single device as shown in fig 2. These sensors are (1) RGB color camera –920×1080 pixels (2) A depth sensor – 512×424 pixels and an infrared sensor – 512×424 pixels [19].

The three sensors generate three streams of data; RGB data from the color camera, depth and skeletal data provided by the depth sensor and Infrared data provided by the infrared sensor. The depth data which is used in this study is immune to color variations, view-point variations, human appearance and lighting conditions [20], [21]. The data is generated at a rate of 30 frames per second. Each frame contains an array containing all the extracted points at the moment of capture.

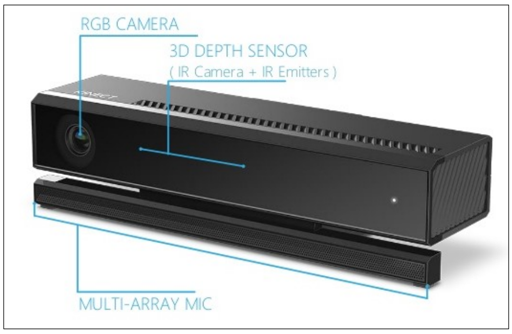

Figure 2. Sensors in Microsoft Kinect.

Originally Microsoft kinect was designed to be used as an Xbox accessory enabling players to interact with the Xbox through body language or voice instead of controllers [19]. According to [20], the sensor has recently become popular for modelling and analysing human motion with various authors [22], [23], [24] confirming its validity for motion capture.

The Kinect's camera coordinates use the infrared sensor to find 3D depth coordinate position of the joints. The positions are provided as distance in meters from the sensor. The origin (x=0, y=0, z=0) is located at the centre of the IR sensor. X coordinate grows to the sensor's left (Subjects right), Y coordinate grows up and Z coordinate grows out in the direction the sensor is facing as shown in fig. 3.

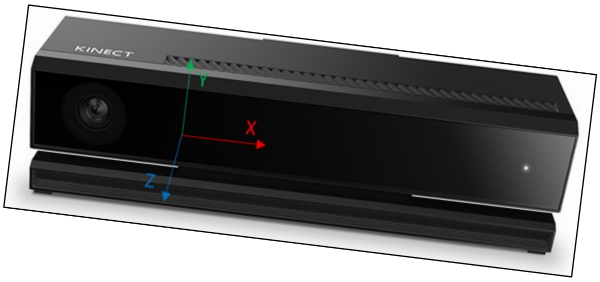

Figure 3. 3D Coordinates of the Kinect Sensor

2) **Kinect for Windows Software Development Kit (SDK) 2.0:** This SDK provides tools and API's that allow programmers to access the data streams (Video, depth and sound) produced by the Kinect sensor on computers running Windows. This study used the kinect studio tool to monitor, record and playback the videos collected by the Kinect sensor. The recorded videos were in .xef file format. Kinect studio uses the skeleton tracking module in the Kinect sensor to provide detailed information about the position and orientation of 25 tracked joints on an individual located in front of the sensor. The position information is provided as a set of 25 three-dimensional skeleton points. Each joint position

is identified by its name (head, shoulders, elbows, wrists, arms, spine, hips, knees, ankles, and so on as illustrated by fig. 4.

3) **Ceska (Cz 75) firearm:** A Ceska pistol loaded with 11 rounds of ammunition was used in the simulation. The pistol had a weight of 2.77kg and a length of 0.2 meters. The firearm was used in the study since it's the most illegally used firearm in Kenya. Authorization to use the firearm was granted by the office of the Inspector General of Police in Kenya.

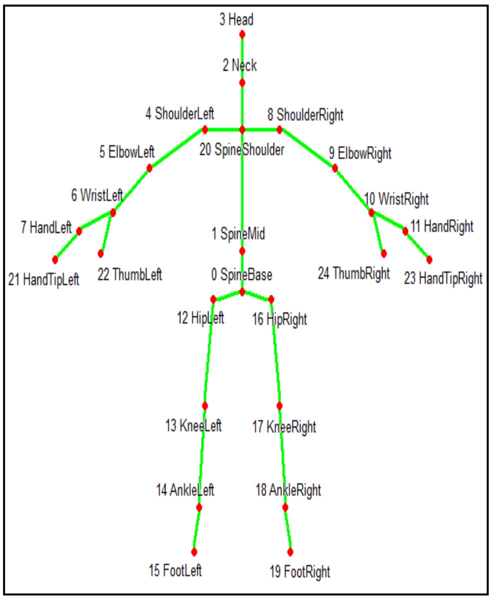

Figure 4. 25 Tracked Joints

4) **Background questionnaire:** Participants responded to a background questionnaire regarding their gender, data of birth, height, weight and whether they had an injury or deformity that affected their walking.

C. Procedure

A simulated recording of persons carrying a concealed firearm was used to gather the required data. This was done in a brightly lit room with a 6 by 1 meters clearly marked path. The Kinect V2 sensor was used to capture the motion of participants. The sensor was connected using a Kinect for windows adapter via USB 3.0 to a laptop with Intel(R) Core(TM)i7-7700HQ CPU @2.80GHZ processor, 16gb RAM and running Windows 10 operating system.

The sensor was elevated 1.2 meters above the ground and 1meter away from the walking path to ensure that the subjects were within the range and field of view of the sensor [15]. A physical marker was placed near the end of the footpath, so that the subjects were aware of where they needed to stop without having to look down which was noted by [25] to skew the results.

All Participants were dressed in trousers and a long jacket or sweater to conceal the firearm. They walked towards the sensor for 4.5 meters in two recorded trials (1) when they were not carrying a firearm (2) When carrying the firearm concealed on the right hip. The videos for all 26 participants were stored and clearly labelled as armed and unarmed. Each recording had an average of 80 frames.

Kinect2 toolbox master adopted from [26] was used to dump the kinect raw data of the 3D skeletal joint position coordinates from the recorded. xef videos into text files. The text files contained the joint numbers (First column), 3D position of the joints (Column 2,3 and 4) and skeleton-tracking state (Column 5). of the skeletal joints which was either Tracked-2, Not Tracked-0, or inferred-1. A sample of the data is illustrated in fig 5.

The acquired skeleton data is based on the Euclidean distance between the sensor and the test subjects and is also dependent on the dimensions of the test subject such as height and limb length [13]. This data can therefore not be used as it is and requires to be normalized.

```
0 -0.392701 -0.215013 2.03281 2
1 -0.375115 0.10818 2.09566 2
2 -0.355986 0.418836 2.14396 2
3 -0.362726 0.561374 2.15985 2
4 -0.540438 0.299046 2.12766 2
5 -0.644968 0.00348408 2.12273 2
6 -0.697195 -0.243969 2.02784 2
7 -0.704174 -0.318604 2.00531 2
8 -0.178403 0.276262 2.10973 2
9 -0.133693 0.00242513 2.07939 1
10 -0.104748 -0.26861 1.94903 1
11 -0.108863 -0.339319 1.91037 1
12 -0.468302 -0.205545 1.99747 2
13 -0.472285 -0.618701 1.93719 2
14 -0.471113 -0.982715 1.89076 2
15 -0.46736 -1.00517 1.73767 1
16 -0.302131 -0.21633 1.99102 2
17 -0.286966 -0.575939 1.80608 2
18 -0.286327 -0.941416 1.79987 2
19 -0.285598 -0.976818 1.65161 1
20 -0.361075 0.342786 2.13435 2
21 -0.698369 -0.396981 1.98987 2
22 -0.669288 -0.346023 1.96881 2
23 -0.112951 -0.416043 1.88915 2
24 -0.140994 -0.346991 1.8814 2
```

Figure 5. Skeletal Joint Position Data

The pair wise relative position-spatial displacement human feature representation technique was used to normalize the data. This technique was adopted from the works of [11], [12], [13] since it was shown to yield data that is more independent with respect to the position between the sensor and the user and the person's specific size. In addition, this study exploits spatial features computed from 3D skeleton coordinates without including the time information in the computation, to make the system independent of the speed of movement [11].

To normalize the distance from the sensor to the test subject according to the pair wise relative position-spatial displacement human feature representation technique, the reference point was moved from the camera to the torso joint of the active test subject by translation. The torso joint was selected as the reference joint since it contains limited movement[11]A normalized joint Ji was achieved as shown Eq 1, where J1 is the torso joint location and ji is the raw joint locations obtained from the Kinect sensor.

$$J_i = j_i - J_1 \quad (1)$$

The invariance of the obtained skeleton data and the test subjects' dimensions according to the pair wise relative position-spatial displacement human feature representation was obtained by scaling with respect to the Euclidean distance (d) between the neck joint (J2) and torso joint (J1). The Euclidean distance formula is the root of the squared differences between two joint vectors as shown in Eq 2. Assuming the torso joint J_1 (x_1, y_1, z_1) and the neck joint is J_2(x_2, y_2, z_2) and is assumed that the distance between joint vector J_1 and J_2 is equal to the distance from vector J_2 to J_1 as shown in Eq 3, the Euclidean distance d is computed as shown in Eq 4.

$$d = \sqrt{(x_2 - x_1)^2 + (y_2 - y_1)^2 + (z_2 - z_1)^2} \quad (2)$$

$$d(J_1, J_2) = d(J_2, J_1) \quad (3)$$

$$d = \sqrt{\sum_{i=1}^{25} (j_2 - J_1)^2} \quad (4)$$

The final normalized 3D joint coordinates (K_i) are computed using Eq 5 by scaling J_i.

$$k_i = \frac{J_i}{||d||},\ 0 \geq i \leq 24 \quad (5)$$

where J_i are the normalized coordinates in Eq 1, and $||d||$ is the Euclidean distance obtained from Eq 4.

The feature f consisting of the normalized joint coordinates is created for each skeleton frame as shown in Eq 6. Two categories of features were generated. One for unarmed scenario and another when participants were armed.

$$f = [k_0, k_1, k_{2,}\ldots\ldots\ldots\ldots\, k_{24}] \quad (6)$$

MATLAB (R2018a) was used for all the computations.

To generate a feature vector (FV), all the features from each frame were combined into a row vector as shown in Eq 7. Where $J1\ x{,}0$ represents the x component of the position of joint $J1$ in frame number 0, $J1\ y{,}0$ and $J1z{,}0$ represent the position of joint J1 in y and z respectively. All joints (1-25) were included in the feature vector resulting to 75 position features representing the 3-Dimension (X, Y, Z) for the 25 tracked joints.

$$FV = \left\{ \begin{array}{c} \left\{ \begin{array}{c} (J0_{X0}, J2_{X0}, \dots\dots\dots J24_{X,0}) \\ (J0_{Y,0}, J1_{Y,0}, \dots\dots . J24_{Y,0}), \\ (J0_{Z,0}, J1_{Z,0}, \dots\dots . J24_{Z,0}) \end{array} \right\} \\ \left\{ \begin{array}{c} (J0_{X,1}, J1_{X,1}, \dots ., J24_{X,1}), \\ (J0_{Y,1}, J1_{Y,1}, \dots\dots . J24_{Y,1}), \\ (J0_{Z,1}, J1_{Z,1}, \dots\dots . J24_{Z,1}) \end{array} \right\} \\ \left\{ \begin{array}{c} . \\ . \\ . \end{array} \right\} \\ \left\{ \begin{array}{c} (J0_{X,n}, J1_{X,n}, \dots ., J24_{X,n}), \\ (J0_{Y,n}, J1_{Y,n}, \dots\dots . J24_{Y,n}), \\ (J0_{Z,n}, J1_{Z,n}, \dots\dots . J24_{Z,n}) \end{array} \right\} \end{array} \right\} \tag{7}$$

Both armed and unarmed features were combined, and a new column was included to classify the features as either armed or unnamed classes. Each feature was considered individually.

This resulted in a row vector with 75*n elements. Where n is the number of frames. A total of 233,325 elements formed the feature vector with 114,225 representing armed and 119,100 unarmed. This feature vector data set is available at fig share.com with the file name Armed and Unarmed.csv.

D. Feature Selection

The generated feature vector described has high dimensionality containing 75 features and over 200,000 instances. Not all these features provided useful information necessary to distinguish between armed and unarmed scenario and may reduce computational efficiency and result in overfitting [27].

To avoid this problem, feature selection algorithms in data mining was used to reduce the dimensionality. The aim of Feature selection is to remove irrelevant and redundant features without any loss of information [27]. Feature selection algorithms are broadly classified into three categories (1) Filter/Ranker-Based, (2) Wrapper (3) Hybrid Method [28].

Ranker-based feature selection algorithms were used in this study due to their generality, high computation efficiency and independence from the classifier [28], [27]. In ranker-based algorithms, all the features are scored and ranked based on certain pre-defined statistical criteria [29], [30]. The scores represent the worth of that feature with respect to the rationale of the algorithm. The features with the highest-ranking values are selected and the low scoring features are removed based on pre-determined threshold [29], [30].

Ranker-based feature selection has been prominently used in various problems. A study by [30] used the technique to determine the intrusion detection factors in a network. A study by [31] used the algorithms for selecting relevant attributes for drought modelling.

The study used the below ranker-based algorithms found in the Waikato Environment for Knowledge Analysis (WEKA) data mining software Version 3.8.2 [32]. The results for all algorithms were compared and the most common features selected.

1) Correlation Feature Ranker Algorithm: The algorithm, proposed by [33], is a probability-based measure that relates variance score of a given class to a feature. According to the algorithm, a good feature has a high attribute-class correlation and low attribute-attribute correlation. The

Correlation score is computed as illustrated in Eq 8 where Where, xi is ith variable,Y is the output class, var() is the variance and cov() denotes covariance

$$R(i) = \frac{cov(x_i,Y)}{\sqrt{var(x_i)*var(Y)}} \quad (8)$$

2) Information Gain: Information Gain is an information theory-based feature ranking technique that measures the dependence between a feature and the class label [30], [34]. A good feature reduces the entropy of a class to the maximum level. Information Gain (IG) of a feature X and the class labels Y is calculated as shown in Eq 9.

$$IG(X,Y) = H(X) - H(X|Y). \quad (9)$$

3) Where Entropy(H) is a measure of the uncertainty associated with a random variable. H(X) and H(X|Y) is the entropy of X and the entropy of X after observing Y , respectively.The maximum value of information gain is 1. A feature with a high information gain is relevant.

4) Gain ratio: Gain ratio is another information theory-based feature ranking technique where the information gain score for a given feature is normalized by the information split value or intrinsic value of the feature. The Information Split or Intrinsic Value is the entropy measure of the attribute. Gain ratio is computed as illustrated in Eq 10.

$$Gain\ Ratio_a = \frac{Info\ Gain_a}{Intrinsic\ Value_a}$$
$$Intrinsic\ Value_a = \sum_{i=1}^{r} -\frac{|a_i|}{N} * \log\left(\frac{|a_i|}{N}\right) \quad (10)$$

Where:

$|a_i|$ – Number of instances where 'a' takes value 'a_i'

N – Number of instances in data set

r – Number of distinct values for 'a'

5) OneR Attribute Evaluator: Evaluates the worth of an attribute by using the OneR classifier. The idea of the OneR (one-attribute-rule) algorithm is to find the one attribute to use that makes fewest prediction errors.

6) Relief-F Algorithm: The original algorithm-Relief was proposed by [35] and uses distance measure between neighboring instances to evaluate features. The algorithm was limited to a scenario where data was divided into binary classes and the algorithm had to distinguish between neighbors. For a given sampled instance, the algorithm randomly selects one neighbor point per class; the neighbor of the same class is called the Hit and the neighbor of a different class is called the Miss for that sample instance.

A good feature is one where the sample has the same value for the 'hit' neighbor and a different value for the 'miss' neighbor [30]. Later, the algorithm evolved to Relief-F to accommodate multi-class scenarios. The Relief-F measure for a given feature 'a' is represented as W[a] is shown in the equation 11:

$$W_a = \frac{1}{k}\left[diff_a(R,H) - \left(\sum_{j=1}^{k} \frac{p(M_j)}{1-p(R)} * diff_a(R,M)\right)\right] \quad (11)$$

where:

$diff_a(R, X)$ – difference in value of 'a' for instances R an

$p(X)$ – probability of X

7) Symmetry uncertainty: Symmetric Uncertainty is another information theory-based feature ranking technique where the information gain score is

normalized by the entropy value of the feature and the class [30]. A good feature is characterized by a high score [34]. The Symmetric Uncertainty score is given by Eq 12.

$$SU_a = 2 * \left(\frac{Info\ Gain_a}{Entropy_a + Entropy_c} \right) \tag{12}$$

E. Threshold Determination for Feature Selection

In order to obtain a subset from ranker feature selection methods, a threshold on the number of features to be selected from the rank-list is required [30]. The features covered by the threshold will be isolated and a dimensionally reduced data set is obtained.

This study used the accuracy plots technique adopted from the works of [30]. The accuracy plot is a graph that plots the number of features on the X-axis against the classification accuracy using that number of features on the Y-axis. The point closest the origin where the slope of the accuracy curve is minimal is the best-suited value for threshold for all the given features [30].

The classification algorithm used in the accuracy plot is not necessarily the algorithm to be used in modelling the problem. The classification algorithm used in this study was the decision tree (C4.5) classifier which is one of the most prevalent and effective algorithms for supervised machine learning and is easy to train [36]. WEKA data mining software was used for the classification.

F. Analysis of Gait Features

Human gait refers to locomotion achieved through the movement of human limbs (Legs and Hands). This section of the analysis used experiments to analyse the features that represent the limbs in the dimensionality reduced data obtained in the previous section, with an aim to distinguishing their position behaviour when participants were armed and unarmed. This would inform the gait characteristics when participants were armed. This was achieved by extracting all Similar features from the dimensionality reduced data that were generated by all the feature selection algorithms and further using paired sampled t-tests to analyse the features that represent the limbs. A significance level $P \leq 0.05$ was used. The Paired Samples t Test uses the repeated measures design to compare two means that are from the same individual, object, or related units with an assumption of normal distribution of the difference between the paired values [37]. The purpose of the test is to determine whether there is statistical evidence that the mean difference between paired observations on a particular outcome is significantly different from zero and did not occur by chance [37]. The selected features representing the limbs were analysed before and after carrying a concealed firearm and their relationship noted. IBM SPSS statistical software V25.0 was used to run the tests. The results of the Paired Samples t Test which represent the relationship between the features was used to describe the distinguishing gait characteristics of participants in the two-test scenario (armed and unarmed) with reference to the anatomical planes of motion. The anatomical planes are hypothetical planes used to transect the human body, in order to describe the location of structures or the direction of movements [38]. In human and animal anatomy, three principal planes are used (1) The sagittal plane or median plane which divides the body into left and right (2) The coronal plane divides the body into back and front (3) The transverse plane which divides the body into head and tail portions [38].

IV. RESULTS

A. Results from Feature Selection

The purpose of the study was to identify gait characteristics drawn from tracked skeletal joint spatial position that are indicative of a person carrying a firearm concealed which tucked on the right hip.

In-order to reduce the dimensionality of the gathered data, the study employed feature ranking algorithms to rank the worth of each feature. The findings are represented below in table 1. The features are ranked in descending order.

Table 1. Ranked Features

Algorithm	Ranked Features
Correlation attribute evaluator	10,11,6,18,19,20,1,2,4,5,12,25,51,21,63,3,45,7,44,43,24,8,54,52,55,23,13,9, 22,65,66,33,48,71,64,47,53,38,29,35,32,70,69,28,34,50,46,57,60,75,49,56,37,58,73,26,27,72,36,68,74,61,59,62,14,4115,31,40,30,16,39,42,17,67
Gain Ratio attribute evaluator	34,47,75,33,32,61,30,59,40,29,10,20,9, 19,4,18,25,43,2,13,44,1,5,11,21,39,22,6,68,45,52,55,8,71,53,54,41,7,3,48,12,51,63,24,23,67,72,73,16,17,66,70,69,14,15,27,65,56,57,42,46,37,49,50,74,36,26, 31,28,64,62,35,60,58,38
Info gain ranking filter	1,13,10,45,11,6,44,4,19,2,8,20,43,18,5, 63,12,25,7,55,21,54,40,39,52,51,53,71, 24,3,22,41,23,34,75,9,48,30,47,33,59, 68,29,61,32,65,64,14,62,42,66,67,73,72,70,69,16,15,58,17,60,31,35,36,37,74,28,27,26,57,46,56,49,50,38
OneR feature evaluator	10,13,1,44,20,45,23,2,4,63,11,55,12,51, 34,21,16,40,65,29,41,9,7,18,5,66,14,25, 19,43,64,49,50,8,73,6,38,15,37,22,62,61,24,52,35,26,57,54,53,74,69,39,59,36, 56,58,48,27,33,3,60,70,42,17,68,67,31, 46,32,75,47,72,28,71,30
Relief F Algorithm	25,23,10,29,9,63,60,18,30,20,12,19,8,24,22,11,14,7,4,35,51,34,16,26,15,49,6,75,39,43,37,74,44,31,38,45,61,47,56,41, 50,27,28,36,40,3,5,59,62,46,1,13,33,21, 64,48,32,68,2,66,55,54,52,65,73,57,53, 71,58,72,70,69,42,67,17
Symmetrical Uncertainty	10,1,13,20,19,4,18,44,2,11,43,25,45,5,,40,8,21,55,7,12,63,34,39,54,52,75,53,71,22,9,51,30,41,3,47,24,33,59,48,23,29, 61,32,68,66,67,35,50,64,65,69,15,46,73,72,70,49,14,62,16,37,28,31,26,36,27,58,17,60,57,42,74,56,38

The features represented in table 1 are serial numbers that represent the features. Table 2 indicates the features that correspond to serial numbers provided by the ranking algorithms. For example, serial 10 represents the X coordinate of joint 9 while 34 represents Y coordinate of joint 8.

To reduce the dimensionality of the feature vector and determine the features that best represent the problem at hand out of the 75 ranked in table 1, an accuracy plot was used and the results and shown in fig. 6.

Table 2. Joint Numbers to Serial number Mapping

Joint Number	Serial Numbers		
	X_{Index}	Y_{Index}	Z_{Index}
0.	1.	26	51
1.	2.	27	52
2.	3.	28	53
3.	4.	29	54
4.	5.	30	55
5.	6.	31	56
6.	7.	32	57
7.	8.	33	58
8.	9.	34	59
9.	10.	35	60
10.	11.	36	61
11.	12.	37	62
12.	13.	38	63
13.	14.	39	64
14.	15.	40	65
15.	16.	41	66
16.	17.	42	67
17.	18.	43	68
18.	19.	44	69

19.	20.	45	70
20.	21.	46	71
21.	22.	47	72
22.	23.	48	73
23.	24.	49	74
24.	25.	50	75

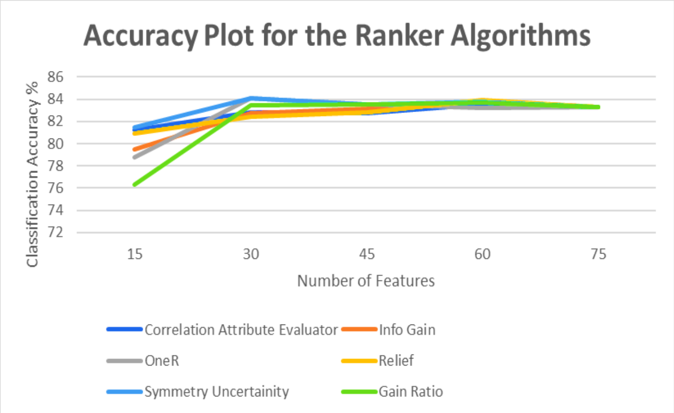

Figure 6. Accuracy Plot

The accuracy plot indicates that 30 features resulted to the most optimum classification accuracy, after which the accuracy is almost constant. Table 3 represents the 30 top ranked features extracted from table 1.

Table 3. Top 30 Ranked Features per algorithm

Algorithm	**30 Ranked Features**
Correlation attribute evaluator	10,11,6,18,19,20,1,2,4,5, 12,25,51,21,63,3,45,7,44,43, 24,8,54,52,55,23,13,9,22,65
Gain Ratio attribute evaluator	34,47,75,33,32,61,30,59,40, 29,10,20,9,19,4,18,25,43,2, 13,44,1,5,11,21,39,22,6,68,45,
Info gain ranking filter	1,13,10,45,11,6,44,4,19,2,8,20, 43,18,5,63,12,25,7,55,21,54,40 ,39,52,51,53,71,24,3,
OneR feature evaluator	10,13,1,44,20,45,23,2,4,63,11 ,55,12,51,34,21,16,40,65,29, 41,9,7,18,5,66,14,25,19,43,
Relief F Algorithm	25,23,10,29,9,63,60,18,30,20, 12,19,8,24,22,11,14,7,4,35,51, 34,16,26,15,49,6,75,39,43,
Symmetrical Uncertainty	10,1,13,20,19,4,18,44,2,11, 43,25,45,5,6,40,8,21,55,7 ,12,63,34,39,54,52,75,53,71,22,

Among the 30 ranked features in the threshold in table 3, 20 common features were extracted and are shown in table 4.

Table 4. Common Features Extracted from table 3

Serial Number	**Joint Axis and Number**	**Joint Name**
10	X-9	Right Elbow
11	X-10	Right Hand
6	X-5	Left Elbow
18	X-17	Right Knee
19	X-18	Right Ankle
20	X-19	Right Foot
1	X-0	Spine Base
2	X-1	Spine Mid
4	X-3	Head
5	X-4	Left Shoulder
12	X-11	Right Hand
25	X-24	Right Thumb
21	X-20	Spine Shoulder
63	Z-12	Left Hip
45	Y-19	Right Foot
7	X-6	Left Wrist
44	Y-18	Right Ankle
43	Y-17	Right Knee

55	Z-4	Left Shoulder
13	X-12	Left Hip

The focus of the study was on human gait which is represented by movement of hand and leg features. From the common ranked features in table 4, features that represent gait were extracted and are shown in table 5.

Table 5. Gait Features

Serial Number	Joint Axis and Number	Joint Name
10	X-9	Right Elbow
11	X-10	Right Hand
6	X-5	Left Elbow
18	X-17	Right Knee
19	X-18	Right Ankle
20	X-19	Right Foot
5	X-4	Left Shoulder
12	X-11	Right Hand
25	X-24	Right Thumb
21	X-20	Spine Shoulder
63	Z-12	Left Hip
45	Y-19	Right Foot
7	X-6	Left Wrist
44	Y-18	Right Ankle
43	Y-17	Right Knee
55	Z-4	Left Shoulder
13	X-12	Left Hip

B. Results from paired sampled t-tests

The paired sample t-test was conducted to determine the relationship between the gait features identified in table 5 in two test scenarios; armed and unarmed. The results of this tests are described below;

i. When subjects were armed, the X-coordinate position of the right elbow was higher ($m= 0.55$, $s=0.68$) than when unarmed ($m= 0.52$, $s=0.63$), $t(1521)=-11.48$ $p \leq 0.05$.

ii. When subjects were armed, the X-coordinate position of the right wrist was higher ($m= 0.56$, $s=0.11$) than when unarmed ($m= 0.52$, $s=0.11$), $t(1521)=-9.38$ $p \leq 0.05$.

iii. When subjects were armed, the X-coordinate position of the right hand was higher ($m= 0.51$, $s=0.13$) than when unarmed ($m= 0.48$, $s=0.13$), $t(1521)=-6.45$ $p \leq 0.05$.

iv. When subjects were armed, the X-coordinate position of the right thumb was higher ($m= 0.49$, $s=0.15$) than when unarmed ($m= 0.45$, $s=0$) , $t(1521)=-5.66$ $p \leq 0.05$.

v. When subjects were armed, the X-coordinate position of the left elbow was lower ($m= -1.03$, $s=0.09$) than when unarmed ($m= -1.00$, $s=0.09$), $t(1521)=8.705$, $p \leq 0.05$.

vi. When subjects were armed, the X-coordinate position of the left shoulder was lower ($m= .0.80$, $s=0.08$) than when unarmed ($m= -0.78$, $s=0.08$) , $t(1521)=7.59$, $p \leq 0.05$.

vii. When subjects were armed, the Z-coordinate position of the left shoulder was slightly lower ($m= 0.32$, $s=0.11$) than when unarmed ($m=0.33$, $s=0.12$), $t(1522)=2.85$, $p \leq 0.05$.

viii. When subjects were armed, the X-coordinate position of the left wrist was lower ($m= -1.06$, $s=0.13$) than when unarmed ($m=-1.03$, $s=0.11$) , $t(1521)=5.56$, $p \leq 0.05$.

ix. When subjects were armed, the X-coordinate position of the left hip was slightly lower ($m= -0.51$, $s=0.04$) than when unarmed ($m=-0.51$, $s=0.41$), $t(1521)=3.387$, $p \leq 0.05$.

x. When subjects were armed, the Y-coordinate position of the left hip was slightly lower ($m= -0.003$, $s=0.03$) than when unarmed ($m=0.003$, $s=0.03$) , $t(1521)=3.252$, $p \leq 0.05$.

xi. When subjects were armed, the X-coordinate position of the right knee was lower ($m= 0.04$, $s=0.26$) than when unarmed ($m= 0.13$, $s=0.34$) , $t(1521)=8.61$ $p \leq 0.05$.

xii. When subjects were armed, the Y-coordinate position of the right knee was lower (m= -1.05, s=0.40) than when unarmed (m= -0.96, s=0.47) , $t(1521)=5.64$ $p \leq 0.05$.

xiii. When subjects were armed, the X-coordinate position of the right foot was lower (m= -0.001, s=0.45) than when unarmed (m= 0.17, s=0.68) , $t(1521)=8.797$ $p \leq 0.05$.

xiv. When subjects were armed, the Y-coordinate position of the right foot was lower (m= -2.19, s=0.70) than when unarmed (m= -2.00, s=0.90) , $t(1521)=6.30$ $p \leq 0.05$.

xv. When subjects were armed, the Y-coordinate position of the right ankle was lower (m= -2.11, s=0.69) than when unarmed (m= -1.94, s=0.89) , $t(1521)=5.90$ $p \leq 0.05$.

V. DISCUSSION OF RESULTS

The findings of this study suggest that carrying a concealed firearm tucked on the right hip has an influence on gait. Among 20 common skeletal joint features shown in table 4, 15 which represent 75% of them are joints that represent the hands and legs as shown in table 5. This is an indication that gait features represented by hands and leg movement are key indicators of a person carrying a concealed firearm tucked on the hip. This is consistent with the findings of [7], [3] who found that a firearm concealed on the hip, resulted in disrupted gait.

A further analysis of the identified gait skeletal joint features using paired sampled t-tests reveal a significant increase in the X-coordinate position of joints that make up the right arm (Elbow, wrist, hand and thumb) when participants were armed with $p \leq 0.05$ and a large t-statistic value. In reference to the anatomical planes of motion, this indicates increased movement on the coronal plane hence signifying arm abduction. This means that when a firearm is tucked on the right hip, the right arm is raised away from the body (Abduction) probably to avoid hitting the firearm tucked on the hip on that side.

Similarly, a significant reduction in x-coordinate position of joints that make up the left arm (Elbow, shoulder, wrist) was observed when participants were armed with $p \leq 0.05$ and a large t-statistic value. This indicates reduced movement along the coronal plane hence signifying arm adduction. This means therefore that when a firearm is tucked on the right hip, there is reduced uplifting of the left arm.

Similarly, there was a significant reduction in the X and Y-coordinate position of skeletal joints that represent the right leg (Knee, foot, ankle) when participants were armed with $p \leq 0.05$ and a large t-statistic value. A reduction in Y joint position indicates reduced movement along the sagittal plane signifying leg extension. This means there is reduced lifting of the right leg probably due to restriction caused by firearm tucked on the right hip. A reduction in the X joint position in this case indicates reduced movement along the coronal plane as a result of leg adduction meaning that the leg was closer to the trunk of the body on that plane.

The empirical results reported herein should be considered in the light of some limitations. First the experiments were conducted in a controlled lab environment which simulated participants carrying a concealed firearm. This environment provided a flat footpath where participants walked in a straight path towards the depth camera. The results may differ in an uncontrolled environment where subjects do not have a pre-defined footpath and may be walking either away from the sensor, to the left of the sensor and to the right of the sensor.

Second, the depth sensor employed in this study (Kinect V2) can track skeletal joints when subjects are a maximum distance of 4.5 meters from the sensor. Any tracking done beyond this distance may yield inconsistent results.

VI. CONCLUSION

The detection of persons carrying a concealed firearm is paramount in maintaining the security in public spaces. The aim of this study was to analyse the gait of persons carrying a concealed firearm tucked on the right hip and to determine the indicative gait characteristics using skeletal tracking and data mining techniques.

In addition to the previously known gait indicators characterized by disrupted stride and reduced arm swing, the study found that carrying a concealed firearm tucked on the right hip additionally resulted in abduction of the right arm, adduction of the left arm and extension and adduction of the right leg.

These findings are beneficial since they extend the findings of related studies highlighted in this paper by providing additional quantitatively derived gait indicators which can be employed by law enforcement officers and CCTV operators who employ behavioural analysis to detect persons carrying concealed firearms.

Future studies can explore scenarios where firearms are concealed on other sides of the hip. For example, on the left hip, back of the hip and at the crouch area. As indicated by [5], this are also potential areas where concealment can be done on the hip.

Various scholars [7], [17] have recommended the automation of concealed firearm detection using computer vision and machine learning techniques. Future studies therefore can employ the optimum skeletal joint features in table 3 to train and develop machine learning models for concealed firearm detection.

VII. REFERENCES

[1]. Gun-Violence-Archive, "past-tolls," Gun Violence Archive, 14 September 2018. [Online]. Available: http://www.gunviolencearchive.org/past-tolls. [Accessed 14 September 2018].

[2]. N. P. Service, "The National Police Service Annual Crime Report 2016," National Police Service, Nairobi, 2016.

[3]. N. C. Meehan and C. Strange, "Behavioral Indicators of Legal and Illegal Gun Carrying," Naval Research Laboratory, Washington, DC, 2015.

[4]. K. Porter, "Characteristics of the armed individual," U.S. Secret Service Publication, Washington, 2010.

[5]. arkchiefs, "Armed Subjects Instructor Guide," September 2017. [Online]. Available: http://arkchiefs.org/wp-content/uploads/2017/08/Armed-Subjects-Instructor-Guide.pdf. [Accessed 20 September 2018].

[6]. S. K. Bandyopadhyay, B. Datta and S. Roy, "Identifications of concealed weapon in a Human," International Journal of Scientific & Engineering Research, pp. 1-7, 2012.

[7]. T. Darker, Blechko and A. G. Gale, "The Role of Emotion Recognition from NonVerbal Behaviour in Detection of Concealed Firearm Carrying," in HUMAN FACTORS and ERGONOMICS SOCIETY 53rd ANNUAL CONFERENCE, 2009.

[8]. H. Gunes, C. Shan, S. Chen and Y. Tian, Emotion Recognition: A Pattern Analysis Approach, Canada: John Wiley & Sons, Inc., 2015.

[9]. I. T. Darker, A. G. Gale and A. Blechko, "CCTV as an automated sensor for firearms detection: Human-derived performance as a precursor to automatic recognision," society of photo-optical

Instrumentation engineers, vol. 7112, pp. 73-80, 2008.

[10]. S. Camalan, G. Sengul, S. Misra, R. Maskeli and R. Damaevi, "Gender Detection using 3D anthropometric measurements by Kinect," Metrology and Measurement Systems, vol. 25, no. 2, pp. 253-267, 2018.

[11]. E. Cippitelli, S. Gasparrini,. E. Gambi and S. Spinsante, "A Human Activity Recognition System Using Skeleton Data from RGBD Sensors," Computational Intelligence and Neuroscience, pp. 1-15, 2016.

[12]. S. Gaglio, G. LoRe and M. Morana, "Human Activity Recognition Process Using 3-D Posture Data," IEEE TRANSACTIONS ON HUMAN-MACHINE SYSTEMS, pp. 586-597, 2015.

[13]. A. Manzi, L. Fiorini, R. Limosani, P. Dario and F. Cavallo, "Two-person activity recognition using skeleton data," IET Computer Vision, pp. 27-35, 2018.

[14]. R. Shrivastava and M. Pandey, "Human Activity Recognition by Analysis of Skeleton Joint Position in Internet of Things (IOT) Environment," Indian Journal of Science and Technology, vol. 10, no. 16, pp. 1-9, 2017.

[15]. C. Tucker, I. Behoora, H. B. Nembhard, M. Lewis, N. W. Sterling and X. Huang, "Machine learning classification of medication adherence in patients with movement disorders using non-wearable sensors," elsevier, pp. 1-15, 2015.

[16]. T. Xu and Y. Zhou, "Fall Detection Based on Skeleton Data," in International Conference on Human Aspects of IT for the Aged Population, Cham, 2017.

[17]. H. Muchiri, I. Ateya and G. Wanyembi, "The Need for Marker," The Need for Marker-Less Computer Vision Techniques for Human Gait Analysis on Video Surveillance to Detect Concealed Firearms, vol. 29, no. 1, pp. 107-118, 2018.

[18]. G. McFassel, S.-J. Hsieh and B. Peng, "Prototyping and evaluation of interactive and customized interface and control algorithms for roboticassistive devices using Kinect and infrared sensor," International Journal of Advanced Robotic Systems, pp. 1-9, 2018.

[19]. N. Khamsemanan, C. Nattee and N. Jianwattanapaisarn, "Human Identification from Freestyle Walks Using Posture-Based Gait Feature," IEEE Transactions on Information Forensics and Security, vol. 13, no. 1, pp. 119-128, 2018.

[20]. L. Tao, P. Adeline, D. Damen, M. Mirmehdi, S. Hannuna, M. Camplani, T. Burghardt and I. Craddock, "A comparative study of pose representation and dynamics modelling for online motion quality assessment," Elsevier, pp. 136-152, 2016.

[21]. F. Han, B. Reily, W. Hoff and H. Zhang, "Space-Time Representation of People Based on 3D Skeletal Data: A Review," Computer Vision and Image Understanding, pp. 85-105, 2015.

[22]. K. Otte, B. Kayser, S. Mansow-Model, J. Verrel, F. Paul, A. U. Brandt and T. Schmitz-H bsch, "Accuracy and Reliability of the Kinect Version 2 for Clinical Measurement of Motor Function," Plos One, pp. 1-17, 2016.

[23]. B. M ller, W. Ilg, M. A. Giese and. N. Ludolph, "Validation of enhanced kinect sensor-based motion capturing for gait assessment," plos one, pp. 1-18, 2017.

[24]. J. Mahvash, B. Alireza and A. Ahmadrez, "A study on validating KinectV2 in comparison of Vicon system as a motion capture system for using in Health Engineering in industry," Nonlinear Engineering, pp. 95-99, 2017.

[25]. S. Liu, X. Meng and C. Tam, "Building information modeling-based building design optimization for sustainability," Energy and Buildings 105, pp. 139-153, 2015.

[26]. Z. Yixin, Z. Yibiao and Z. Song-Chun, "Understanding Tools: Task-Oriented Object Modeling, Learning and Recognition," in IEEE Conference on Computer Vision and Pattern

Recognition (CVPR), Boston, Massachusetts, 2015.
[27]. K. Sutha and J. Tamilselvi, "A Review of Feature Selection Algorithms for Data Mining Techniques," International Journal on Computer Science and Engineering (IJCSE), pp. 63-67, 2015.
[28]. K. Pavya and B. Srinivasan, "Feature Selection Techniques in Data Mining: A Study," International Journal of Scientific Development and Research (IJSDR), pp. 594-598, 2017.
[29]. B. Kumari and T. Swarnkar, "Filter versus Wrapper Feature Subset Selection in Large Dimensionality Micro array: A Review," International Journal of Computer Science and Information Technologies, pp. 1048-1053, 2011.
[30]. K. K. Vasan and B. Surendiran, "Feature subset selection for intrusion detection using various rank-based algorithms," International journal of Computer Applications in Technology, pp. 298-307, 2017.
[31]. G. B. Demisse, T. Tadesse and Y. Bayissa, "Data Mining Attribute Selection Approach for Drought Modelling: A Case Study For," International Journal of Data Mining & Knowledge Management Process (IJDKP), pp. 1-16, 2017.
[32]. M. Hall, E. Frank, G. Holmes and B. Pfahringer, "The WEKA Data Mining Software: An Update," SIGKDD Explorations, p. 10.18, 2005.
[33]. M. A. Hall, "Correlation-based feature selection for discrete and numerical class machine learning," in 17th International Conference on Machine Learning, Stanford, 2000.
[34]. Z. Zhao, S. Sharma, A. Anand, F. Morstatter, S. Alelyani and H. Liu, "Advancing Feature Selection Research ASU Feature Feature Selection Repository," Arizona State University, Arizona, 2010.
[35]. K. Kira and L. A. Rendell, "A practical approach to feature selection," in Proceeding ML92 Proceedings of the ninth international workshop on Machine learning, Aberdeen, 1992.
[36]. B. N. Lakshmi, T. S. Indumathi and N. Ravi, "A study on C.5 Decision Tree Classification Algorithm for Risk Predictions during Pregnancy," in International Conference on Emerging Trends in Engineering, Science and Technology (ICETEST- 2015), Kerala, 2015.
[37]. T. K. Kim, "T test as a parametric statistic," Korean Journal of Anesthesiology, pp. 540-546, 2015.
[38]. B. Basu, Biomaterials for Musculoskeletal Regeneration: Concepts, Bangalore: Springer, 2016.

Cite this article as :

Henry Muchiri, Ismail Ateya, Gregory Wanyembi, "Human Gait Indicators of Carrying a Concealed Firearm : A Skeletal Tracking and Data Mining Approach", International Journal of Scientific Research in Computer Science, Engineering and Information Technology (IJSRCSEIT), ISSN : 2456-3307, Volume 3 Issue 8, pp. 368-383, November-December 2018.

Available at doi : https://doi.org/10.32628/CSEIT1838106

Journal URL : http://ijsrcseit.com/CSEIT1838106